Quantum Monte Carlo simulation of the one-dimensional spin S xxz model. I. The method

1985 J. Phys. A: Math. Gen. 18 2479

(http://iopscience.iop.org/0305-4470/18/13/024)

J. Phys. A: Math. Gen. 18 (1985) 2479-2496. Printed in Great Britain

Quantum Monte Carlo simulation of the one-dimensional spin S xxz model: I. The method

Mihail Marcu and Andreas Wiesler†

Fakultät für Physik, Universität Freiburg, Hermann-Herder-Strasse 3, D-7800 Freiburg, West Germany

Received 1 March 1984, in final form 19 March 1985

Abstract. We develop a quantum Monte Carlo procedure for the xxz spin chain. The quantum model in one dimension is mapped by a path integral method based on the Trotter formula into the infinite anisotropy limit of a classical two-dimensional spin system. The expectation values of the energy density, susceptibility and static s^z-s^z structure function are computed in the classical model for finite but increasing anisotropy. The computation method is a Monte Carlo simulation of the classical system. The results are systematically extrapolated to the infinite anisotropy limit.

1. Introduction

In this paper we continue the investigation, begun in Wiesler (1982), of the quantum Monte Carlo method using the Trotter formula (Trotter 1959, Suzuki 1976). We consider the quantum statistical mechanics of the xxz model, defined by the following Hamiltonian

$$H = -\sum_{i=1}^{N} (S_i^x S_{i+1}^x + S_i^y S_{i+1}^y + J_z S_i^z S_{i+1}^z). \tag{1.1}$$

S_i^x, S_i^y, S_i^z are the generators of SU(2) at the site i, N is the number of lattice sites of the chain and J_z is a coupling constant. For spin-$\frac{1}{2}$, H can be diagonalised exactly (des Cloizeaux and Gaudin 1966). Let H be a sum of n operators:

$$H = H_1 + H_2 + \ldots + H_n. \tag{1.2}$$

The Trotter formula states that (β is the inverse of the temperature T):

$$e^{-\beta H} = \lim_{M\to\infty} [\exp(-\beta H_1/M) \exp(-\beta H_2/M) \ldots \exp(-\beta H_n/M)]^M. \tag{1.3}$$

By inserting complete sets of states on the RHS of (1.3), we can rewrite the partition function into the partition function of a two-dimensional highly anisotropic classical model. Similarly, we can rewrite the expectation value of an operator A,

$$\langle A\rangle_N = \mathrm{Tr}\, A \exp(-\beta H)/\mathrm{Tr} \exp(-\beta H) \tag{1.4}$$

into an expectation value of an operator in the classical two-dimensional system. At this stage the use of a Monte Carlo procedure becomes possible. However, there are

† Present address: SPACETEK GMBH, D-7800 Freiburg, West Germany.

0305-4470/85/132479+18$02.25

two effects which make this difficult. Firstly, if M is very large, the couplings of the classical model will take extreme values, and as a consequence the errors in the Monte Carlo computation will be large. Secondly, if M is not large enough, the results will not be close to the $M \to \infty$ limit.

The first attempt to use the Trotter formula in a quantum Monte Carlo simulation was made by Suzuki (1976, 1977). Our Monte Carlo procedure was described partly in Honerkamp (1982), where a preliminary account of our work is given. Initially our goal has been to investigate the $M \to \infty$ limit 'experimentally', i.e. by computing the same expectation values for increasing M, until the results stabilise. We later discovered, however, that for large enough M the expectation values are linear in $1/M^2$. This allows for a systematic extrapolation procedure. A rigorous proof for the linearity in $1/M^2$ will be given elsewhere.

In § 2 we derive a classical two-dimensional model for general spin S on an $N \times M$ lattice by taking a finite value of M in (1.3). Then we discuss the question of what quantities can be computed using a Monte Carlo procedure for this classical spin system. The Monte Carlo procedure itself is described in § 3. In § 4 we give our spin-1 results for the energy density, magnetic susceptibility and s^z-s^z static correlation function. We took five different values for the coupling J_z. The number of lattice sites was $N = 20$ throughout the whole computation and no attempt was made to investigate the thermodynamic limit $N \to \infty$. However, we expect problems with the thermodynamic limit only at very low temperatures, especially in the isotropic ferromagnet and the isotropic antiferromagnet cases. Our goal in this paper was to investigate the quantum Monte Carlo method itself. High precision calculations for general values of the spin S will be given in a subsequent publication. Our conclusions and outlook are contained in § 5.

2. The classical two-dimensional spin system

Following Barma and Shastry (1978), let us split H into four parts:

$$\begin{aligned} H &= H_1 + H_2 + H_3 + H_4 \\ H_1 &= -\sum_{i=\text{even}} (S_i^x S_{i+1}^x + S_i^y S_{i+1}^y + S_i^z S_{i+1}^z) \\ H_3 &= -\sum_{i=\text{odd}} (S_i^x S_{i+1}^x + S_i^y S_{i+1}^y + S_i^z S_{i+1}^z) \\ H_4 &= H_2 = -\tfrac{1}{2}(J_z - 1) \sum_{\text{all } i} S_i^z S_{i+1}^z . \end{aligned} \tag{2.1}$$

We will take an even lattice size N and periodic boundary conditions. Now we use the Trotter formula (M is even):

$$\begin{aligned} Z_N &= \operatorname{Tr} \exp(-\beta H) = \lim_{M \to \infty} Z_{N,M} \\ Z_{N,M} &= \operatorname{Tr}[\exp(-2\beta H_1/M) \exp(-2\beta H_2/M) \exp(-2\beta H_3/M) \exp(-2\beta H_4/M)]^{M/2} . \end{aligned} \tag{2.2}$$

The classical two-dimensional model is obtained by inserting M complete sets of intermediate states in (2.2). These states are chosen as eigenstates of the S_i^z operators. It is crucial that H_1, H_2, H_3 and H_4 are sums over commuting local operators.

$Z_{N,M}$ is now the partition function of a classical spin system on an $N \times M$ chessboard lattice. The spins $s_{ij} \in \{-S, -S+1, \ldots, S-1, S\}$ are located at the lattice sites, and the interaction takes place on the 'even' plaquettes (the hatched plaquettes of figure 1). The partition function is

$$Z_{N,M} = \sum_{s} \prod_{\substack{i=1,\ldots,N \\ j=1,\ldots,M \\ i+j=\text{even}}} f(s_{ij}, s_{i+1\,j}, s_{ij+1}, s_{i+1\,j+1}) \tag{2.3}$$

with the plaquette weights (for notation see also figure 2):

$$f(s_1, s_2, s_1', s_2') = \exp[\bar{\beta}(J_z - 1)(s_1 s_2 + s_1' s_2')]$$
$$\times \sum_{\sigma=0}^{2S} C^{\sigma\, S_1+S_2}_{S_{s_1}, S_{s_2}} C^{\sigma\, S_1+S_2}_{S_{s_1'}, S_{s_2'}} \exp\{\bar{\beta}[\sigma(\sigma+1) - 2S(S+1)]\}. \tag{2.4}$$

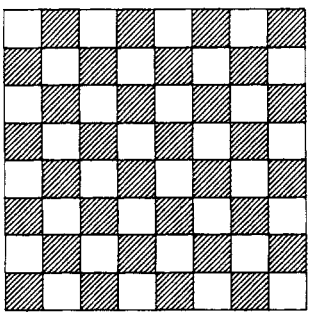

Figure 1. The chessboard lattice, with the even plaquettes hatched.

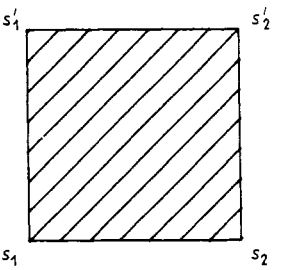

Figure 2. An even (interacting) plaquette.

Here $\bar{\beta} = \beta/M$ and C are the SU(2) Clebsch-Gordan coefficients. In table 1 we list the plaquette weights for $S = \frac{1}{2}$ and $S = 1$.

In equation (2.4) the plaquette weight is zero unless

$$s_1 + s_2 = s_1' + s_2'. \tag{2.5}$$

This is a consequence of the conservation of the z component of the total spin. The up-down (i.e. reflection in the xy plane) symmetry implies

$$f(s_1, s_2, s_1', s_2') = f(-s_1, -s_2, -s_1', -s_2') \tag{2.6}$$

and spatial parity and Hermiticity of H imply

$$f(s_1, s_2, s_1', s_2') = f(s_2, s_1, s_2', s_1') = f(s_1', s_2', s_1, s_2). \tag{2.7}$$

Equation (2.5) allows for a particle interpretation in the Feynman path integral sense. The world lines of the particles move in the 'Trotter' or 'Euclidean time' direction. At the lattice site (i, j) there are $s_{ij} + S$ world lines. A world line bit lies either on a vertical (timelike) link or on the diagonal of an even plaquette, as shown in table 1 for $S = \frac{1}{2}$ and $S = 1$. Two lines never cross and there are at most $2S$ lines on the same vertical link or on the same diagonal of an even plaquette. In figures 3 and 4 several configurations are drawn using both spins and world lines of particles. A configuration

Table 1. Allowed configurations of an even plaquette in terms of spins and world lines of particles, and the corresponding plaquette weights.

	Weight	Configurations having this weight
$S=\frac{1}{2}$	$e^{J_z\bar{\beta}/2}$	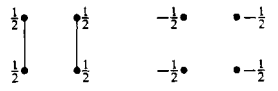
	$e^{-J_z\bar{\beta}/2}\cosh\bar{\beta}$	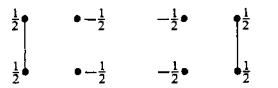
	$e^{-J_z\bar{\beta}/2}\sinh\bar{\beta}$	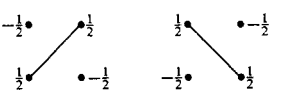
$S=1$	$e^{2J_z\bar{\beta}}$	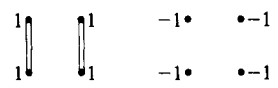
	$\cosh(2\bar{\beta})$	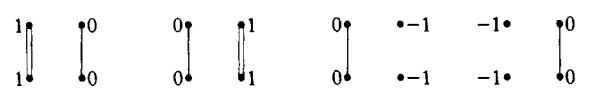
	$\sinh(2\bar{\beta})$	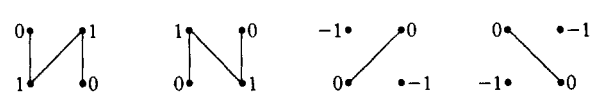
	$\frac{1}{6}e^{-2J_z\bar{\beta}}(e^{4\bar{\beta}}+3+2e^{-2\bar{\beta}})$	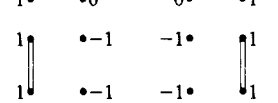
	$\frac{1}{3}(2e^{2\bar{\beta}}+e^{-4\bar{\beta}})$	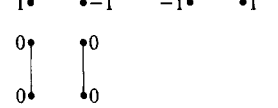
	$\frac{2}{3}e^{-J_z\bar{\beta}}\sinh(3\bar{\beta})$	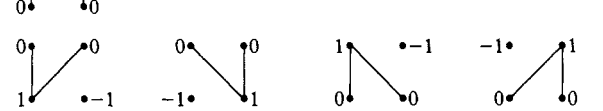
	$\frac{1}{6}e^{-2J_z\bar{\beta}}(e^{4\bar{\beta}}-3+2e^{-2\bar{\beta}})$	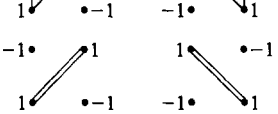

has a fixed particle number n_p defined as the number of world lines minus $N\times S$:

$$n_p=\sum_{i=1}^{N} s_{ij}. \tag{2.8}$$

n_p is independent of j. Because of the periodic boundary conditions, the world lines can wind around the lattice in space direction. A configuration has a fixed winding number n_w:

$$n_w=\sum_{j=1}^{M}(-1)^{i+j}s_{ij} \tag{2.9}$$

n_w is independent of i.

Now let us see what quantities of interest for the xxz model can be computed using the classical model with partition function $Z_{N,M}$. We shall discuss four types of

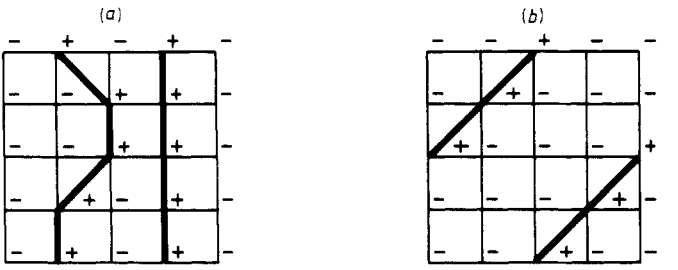

Figure 3. Two configurations for $S=\frac{1}{2}$; '+' means '$\frac{1}{2}$', '−' means '$-\frac{1}{2}$'. $N=4$, $M=4$. (*a*) $n_p=0$, $n_w=0$; (*b*) $n_p=-1$, $n_w=1$.

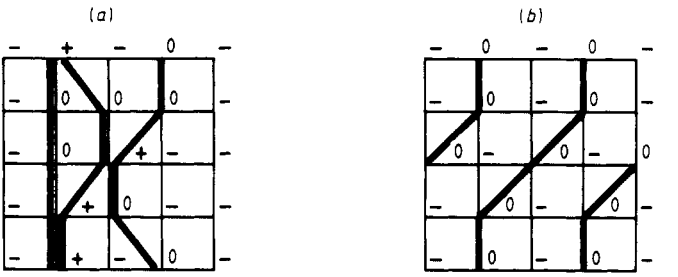

Figure 4. Two configurations for $S=1$, '+' means '1', '−' means '−1'. $N=4$, $M=4$. (*a*) $n_p=-1$, $n_w=0$; (*b*) $n_p=-2$, $n_w=1$.

quantities. Let us denote by $f(p)$ the weight (2.4) of the plaquette p; $p=$even consequently means an interacting plaquette.

2.1. Thermodynamic quantities

Let us take two examples. The energy density e_N is

$$e_N=-\frac{1}{N}\frac{\partial \ln Z_N}{\partial \beta}=-\lim_{M\to\infty}\frac{1}{NM}\frac{\partial \ln Z_{N,M}}{\partial \bar{\beta}}$$

$$=-\lim_{M\to\infty}\frac{1}{Z_{N,M}}\sum_s\left(\frac{1}{NM}\sum_{p=\text{even}}e(p)\right)\prod_{p'=\text{even}}f(p') \tag{2.10}$$

with

$$e(p)=(\partial/\partial\bar{\beta})\ln f(p). \tag{2.11}$$

The magnetisation density is

$$m_N=\frac{1}{N}\frac{1}{Z_N}\operatorname{Tr}\left(\sum_{i=1}^{N}S_i^z\right)\exp(-\beta H)=\lim_{M\to\infty}\frac{1}{Z_{N,M}}\sum_s\frac{n_p}{N}\prod_{p=\text{even}}f(p). \tag{2.12}$$

2.2. Equal time expectation values of products of S_i^z operators

As an example take the s^z-s^z correlation function C:

$$C(r)=\frac{1}{Z_N}\operatorname{Tr}S_i^zS_{i+r}^z\exp(-\beta H)=\lim_{M\to\infty}\frac{1}{Z_{N,M}}\sum_s\left(\frac{1}{MN}\sum_{i,j}s_{ij}s_{i+r\,j}\right)\prod_{p=\text{even}}f(p). \tag{2.13}$$

Its Fourier transform is the static structure function $I(q)$:

$$I(q) = \sum_{r=1}^{N} C(r) \exp(-iqr), \qquad q = 2\pi k/N, \qquad k = 1, \ldots, N. \tag{2.14}$$

The magnetic susceptibility is related to $I(0)$:

$$\chi_N^{zz} = \beta I(0) = \beta \lim_{M\to\infty} \frac{1}{Z_{N,M}} \sum_s \frac{n_p^2}{N} \prod_{p=\text{even}} f(p). \tag{2.15}$$

2.3. Expectation values of operators which do not commute with all S_i^z

For example, the dynamical structure function or the s^x-s^x correlation function. These quantities cannot be computed directly with our Monte Carlo method. In the case of the s^x-s^x correlation function, we could insert in (2.2) complete sets of eigenstates of the S_i^x rather than the S_i^z, and then derive a new classical two-dimensional system. This will be done in a subsequent publication. For the dynamical structure function there is as yet no method available.

2.4. Energy differences between two eigenvalues of H

This can be computed by analysing the Euclidean time decay of appropriately chosen operators in the limit $T \to 0$. This method plus renormalisation group considerations are used in Schmatzer (1983) and Marcu and Schmatzer (1985) to compute masses of two-particle states in the Thirring model.

3. The quantum Monte Carlo method

The quantum Monte Carlo method consists of two steps. First, one has to perform a Monte Carlo calculation for the classical system derived in § 2. Then one has to perform the $M \to \infty$ limit.

The Monte Carlo procedure for the classical system is complicated by the constraint (2.5) on the admissible configurations. As seen in Cullen and Landau (1983), it is unpractical to produce configurations without any restriction, and then throw away the undesired ones. On the other hand, all admissible configurations should be allowed to occur unless there is some well founded reason to drop some of them.

Starting from a given admissible configuration of the classical system with particle number n_p and winding number n_w all other admissible configurations with the same n_p and n_w can be reached by the following local procedure. Consider the odd plaquette ABCD and its four even neighbours as shown in figure 5. Equation (2.5) requires

$$\begin{aligned} &s_A + s_{A'} = s_C + s_{C'}, \qquad && s_A + s_B = s_{A''} + s_{B''}, \\ &s_B + s_{B'} = s_D + s_{D'}, \qquad && s_C + s_D = s_{C''} + s_{D''}. \end{aligned} \tag{3.1}$$

The transformation

$$s_A \to s_A + s_0, \qquad s_B \to s_B - s_0, \qquad s_C \to s_C + s_0, \qquad s_D \to s_D - s_0 \tag{3.2}$$

with s_0 chosen such that all new values are admissible, preserves the conditions (3.1).

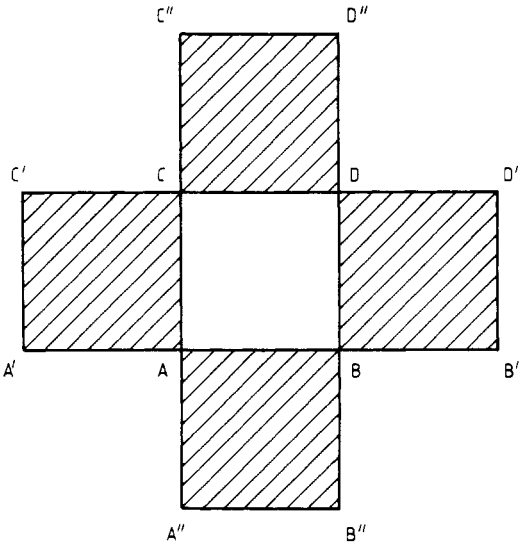

Figure 5. The odd plaquette ABCD and its four even neighbouring plaquettes.

The first part of our Monte Carlo algorithm consists in making sweeps through the lattice and offering the transformation (3.2) at each odd plaquette.

In order to change the particle number we made sweeps through the spatial lattice and at each point offered to insert or remove straight world lines. Technically, this is achieved by the transformation (i is a fixed point in the spatial lattice)

$$s_{ij} \to s_{ij} + \sigma_i \qquad j = 1, \ldots, M \tag{3.3}$$

with σ_i chosen such that all new values are admissible.

Similarly, the winding number can be changed by the transformation

$$s_{ij} \to s_{ij} + (-1)^{i+j}\sigma_j \qquad i = 1, \ldots, N. \tag{3.4}$$

As $\bar{\beta} \to 0$ the classical model becomes highly anisotropic (this can be seen by expanding the plaquette weights in $\bar{\beta}$). One consequence is that the configurations with $n_w \neq 0$ are suppressed by a factor of at least $\exp(-n_w \bar{\beta} N)$ relative to the configurations with $n_w = 0$. Therefore they almost never occur. After checking in test simulations that this is indeed so, we decided to fix $n_w = 0$ for our computations. A 'sweep' will consist of a sweep of local transformations followed by a sweep of transformations (3.3).

The $S = \frac{1}{2}$ case has also been investigated by Hirsch *et al* (1982). They used, however, only a local algorithm similar to ours in order to 'bend' world lines, leaving the particle number constant and equal to zero (equivalently they took the total spin in the z direction equal to zero). Using (2.15) we see that this leads to the susceptibility χ^{zz} being identically zero. In fact the particle number statistics can be used as a check for the accuracy of the calculation. If the particle number is not distributed symmetrically around zero (for one-dimensional xxz models without a magnetic field there is no magnetisation at finite temperatures), we know that we have not done enough sweeps through the lattice.

For the isotropic ferromagnet, the particle number fluctuations are largest since there is a ground state for each value of n_p. In figure 6 we show the particle number

statistics for 5000 sweeps (after a warm-up of 2500 sweeps), $S=1$, $J_z=1$, and the inverse temperatures $\beta=1$, $\beta=1.5$, $\beta=2.5$ and $\beta=5$. For each value of β several values of M were taken. At low temperatures the particle number fluctuates wildly, as expected for the isotropic ferromagnet, and we would need many more sweeps for an accurate result. Notice that in figure 6(*c*) the symmetry of the distribution of n_p around zero becomes worse as M increases.

After having computed the expectation value of some quantity for fixed J_z and β but for several values of M, we need an extrapolation procedure in order to get the

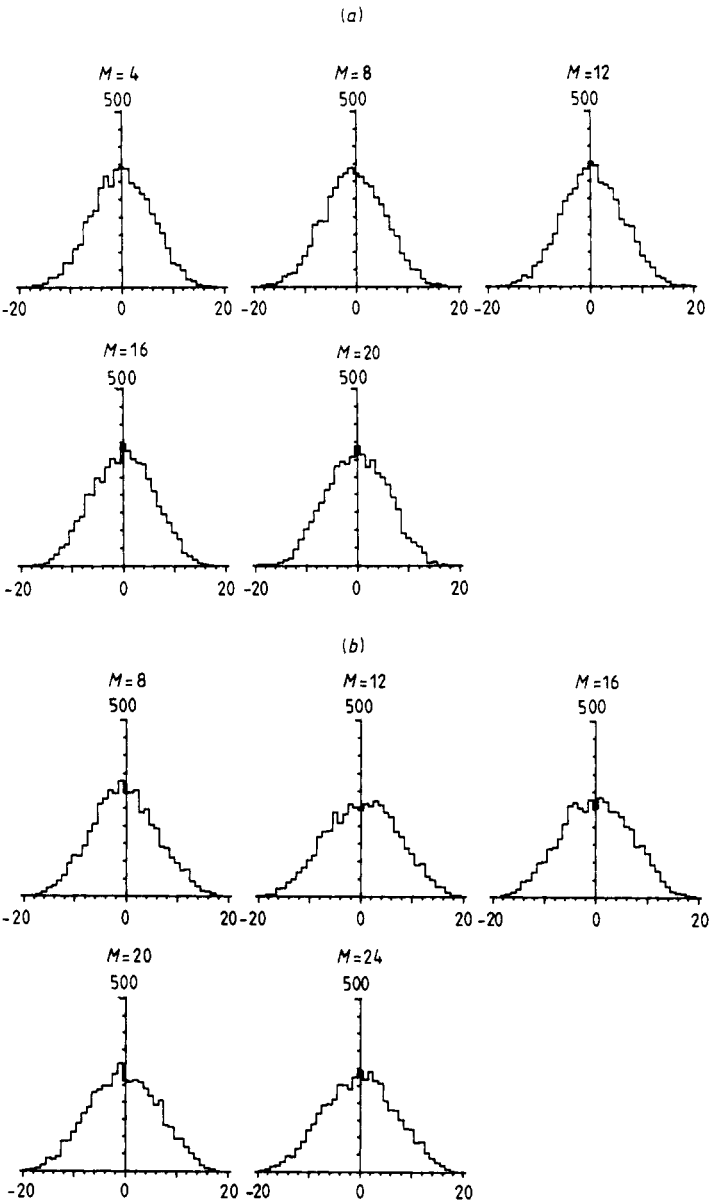

Figure 6.

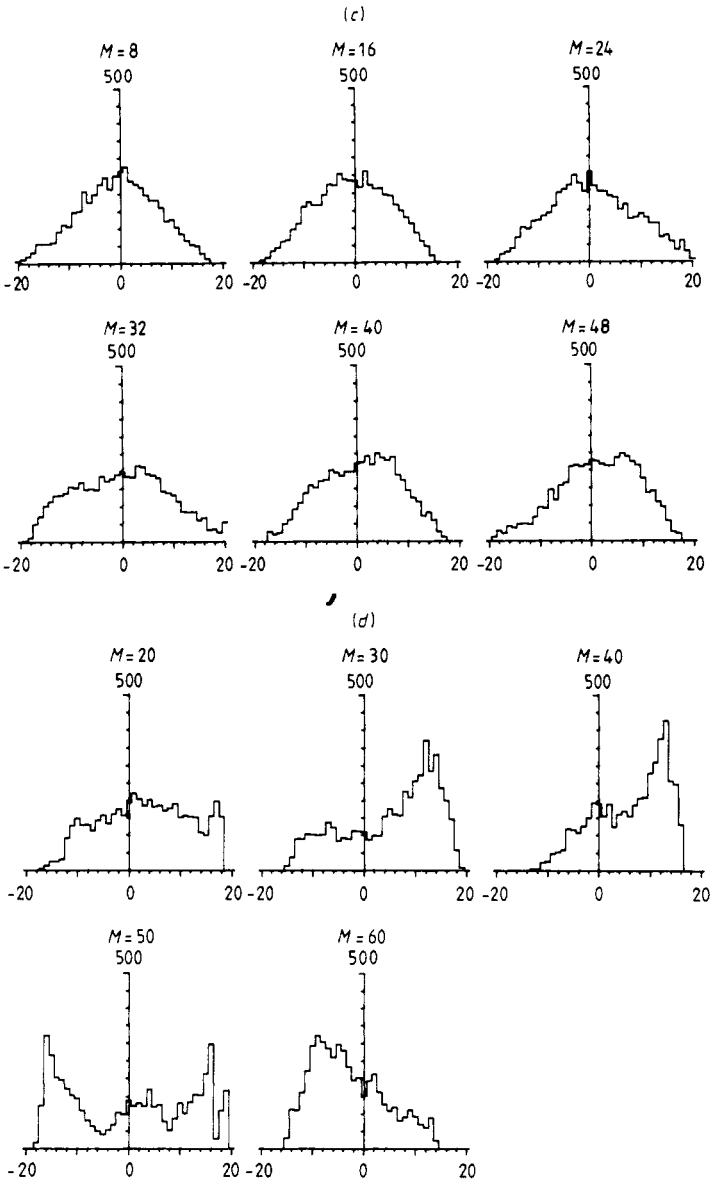

Figure 6. Multiplicity (y axis) taken by the particle number n_p (x axis) for the isotropic ferromagnet in a sample of 5000 configurations. (a) $J_z = 1.0$, $\beta = 1.0$; (b) $J_z = 1.0$, $\beta = 1.5$; (c) $J_z = 1.0$, $\beta = 2.5$; (d) $J_z = 1.0$, $\beta = 5.0$. $N = 20$.

$M \to \infty$ result which interests us. At the beginning we increased the value of M until it was apparent that the expectation value had stabilised. The results of such a calculation for $S = 1$ are given in figures 7(a) for the energy density, and 7(b) for $I(\pi/2)$. The number of sweeps was the same as above, with a measurement done after each sweep. For $J_z = 1$, $\beta = 2.5$ and for $J_z = 1$, $\beta = 5$, the results for $I(\pi/2)$ are unreliable, as expected from figure 6. The energy results are however reasonable, because for the isotropic ferromagnet at low temperatures the energy is not very sensitive to fluctuations

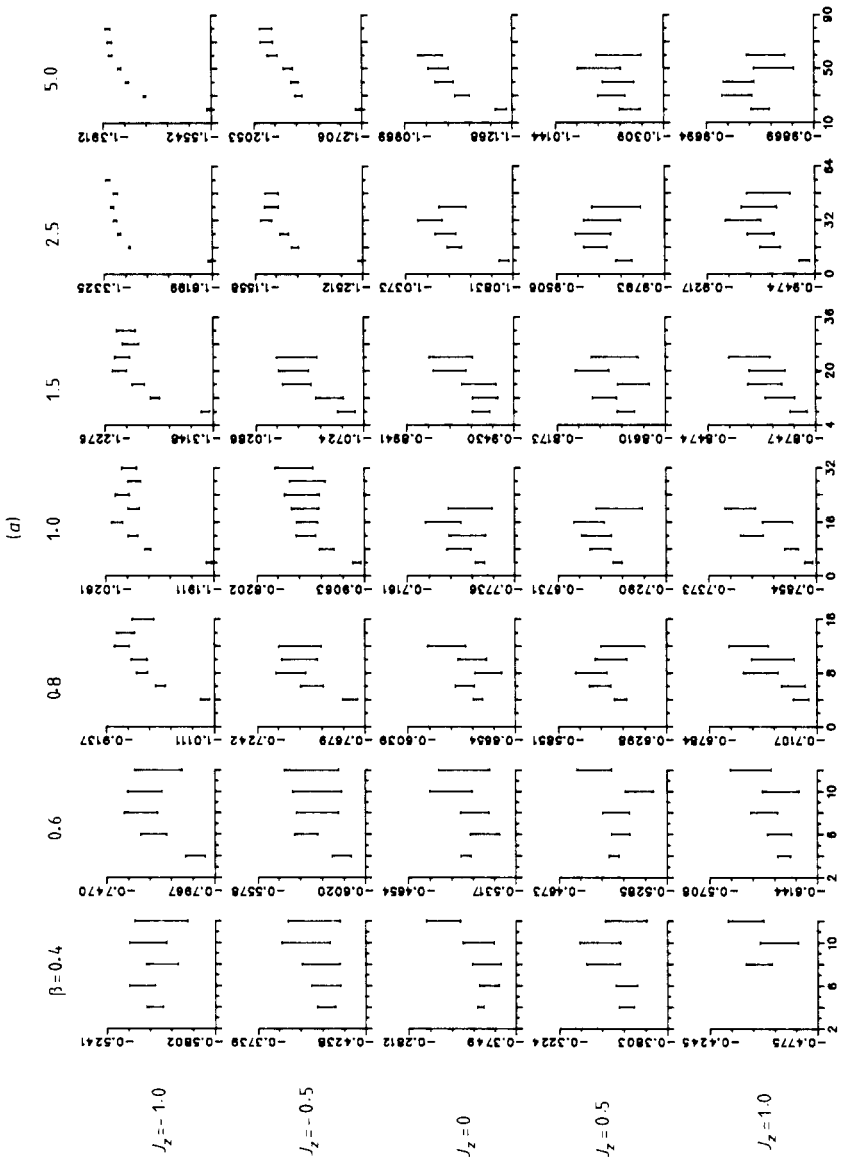
(a)
β = 0.4
0.6
0.8
1.0
1.5
2.5
5.0
$J_z = -1.0$
$J_z = -0.5$
$J_z = 0$
$J_z = 0.5$
$J_z = 1.0$

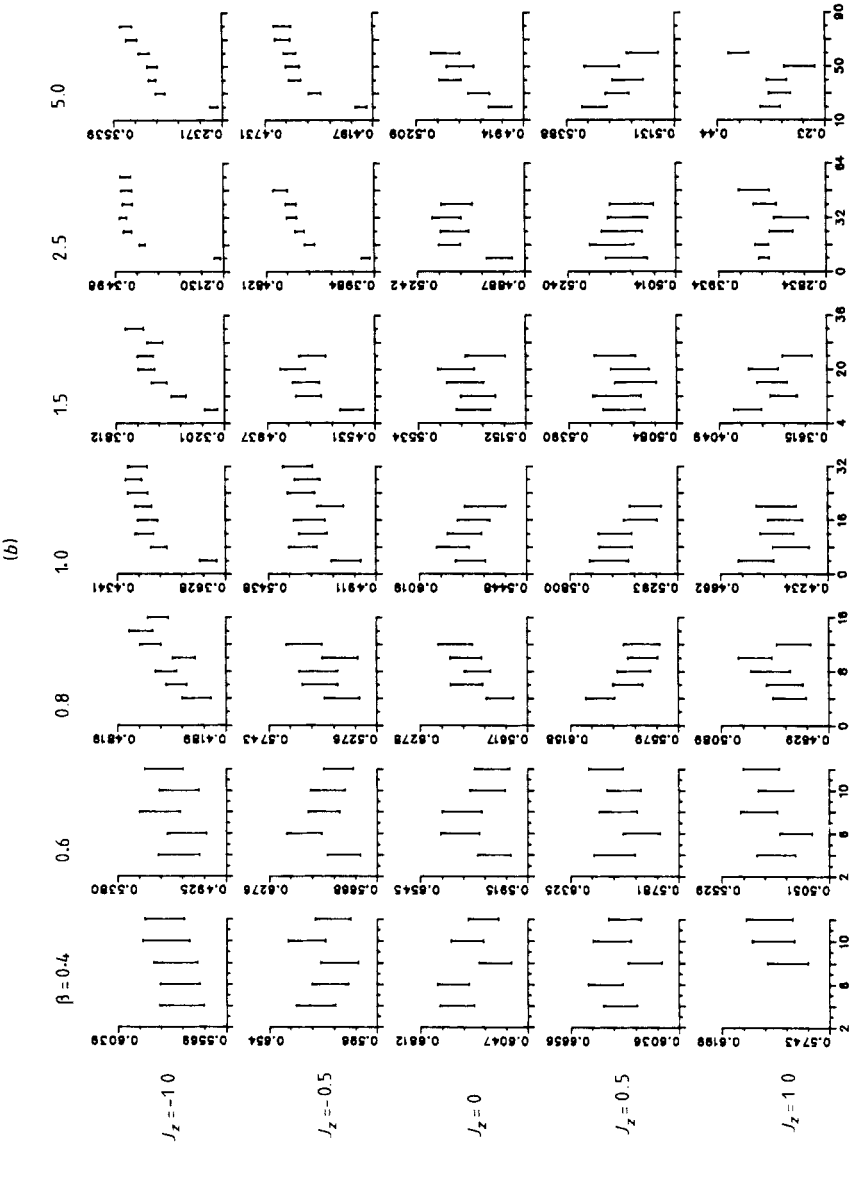

Figure 7. (*a*) Energy density, and (*b*) $I(\pi/2)$ plotted against M. The error bars for the data points are given at a confidence rate of 68%.

in particle number. Notice also that although the number of sweeps was always 5000, the errors in the data points for the energy are increasing with M. For $I(\pi/2)$ this does not happen.

The value of M cannot be increased beyond a certain limit. If $M \to \infty$, then $\bar{\beta} \to 0$, and for very small values of $\bar{\beta}$ some plaquette weights are close to one while others are almost zero (see (2.4) and table 2). In fact, for $\bar{\beta} \to 0$ only the weights of configurations with straight particle lines are not very small. As $\bar{\beta}$ becomes very small the Monte Carlo simulation becomes increasingly inefficient. For both this reason and computer time economy, it is desirable to extrapolate the $M \to \infty$ results from as low values of M as possible.

Table 2. (a) The Monte Carlo results for the energy density and (b) ground-state energy density (from Blöte 1975).

(a)

J_z		$\beta = 0.4$	0.6	0.8	1.0	1.5	2.5	5.0
−1.0	Energy density	−0.5471	−0.7589	−0.9280	−1.0552	−1.2353	−1.3477	−1.3901
	Error	0.0159	0.0137	0.0088	0.0085	0.0074	0.0067	0.0047
−0.5	Energy density	−0.4004	−0.5746	−0.7349	−0.8593	−1.0423	−1.1693	−1.2122
	Error	0.0158	0.0138	0.0110	0.0097	0.0106	0.0057	0.0038
0	Energy density	−0.3396	−0.5050	−0.6374	−0.7414	−0.9193	−1.0507	−1.1027
	Error	0.0205	0.0187	0.0132	0.0127	0.0130	0.0063	0.0046
0.5	Energy density	−0.3510	−0.5030	−0.6016	−0.6926	−0.8368	−0.9609	−1.0223
	Error	0.0150	0.0126	0.0108	0.0107	0.0115	0.0065	0.0047
1.0	Energy density	−0.4511	−0.5928	−0.6936	−0.7631	−0.8593	−0.9331	−0.9765
	Error	0.0159	0.0107	0.0087	0.0070	0.0075	0.0045	0.0047

(b)

J_z	−1.0	−0.5	0	0.5	1.0
Ground-state energy density	−1.403	−1.230	−1.1162	−1.0417	−1.0

It turns out that for high enough values of M the expectation values are linear in $1/M^2$. For a local observable A (cf equations (1.4), (2.2))

$$\langle A \rangle_{N,M} = \langle A \rangle_N + \text{constant} \times 1/M^2 + O(1/M^3) \tag{3.5}$$

with the constant on the RHS depending on A, β and N. Equation (3.5) also holds for sums of local and bilocal observables such as the quantities described in § 2. A more detailed theoretical argument leading to (3.5) will be given elsewhere.

Equation (3.5) suggests a linear fit of the data points as a function of $1/M^2$ to be a suitable extrapolation procedure for $M \to \infty$. In figure 8 we show two linear fits to the energy density data. In figure 8(a) the linear fit of all data points (broken line) is not good. If we disregard the smallest value of M, the linear fit becomes satisfactory (dotted line). Thus the $1/M^3$ correction to (3.5) can be neglected for all data points except that corresponding to the smallest value of M. In figure 8(b) both the broken and the dotted lines are good linear fits. Notice that the estimated error for the extrapolated value is smaller for the broken line than for the dotted line. Thus it is

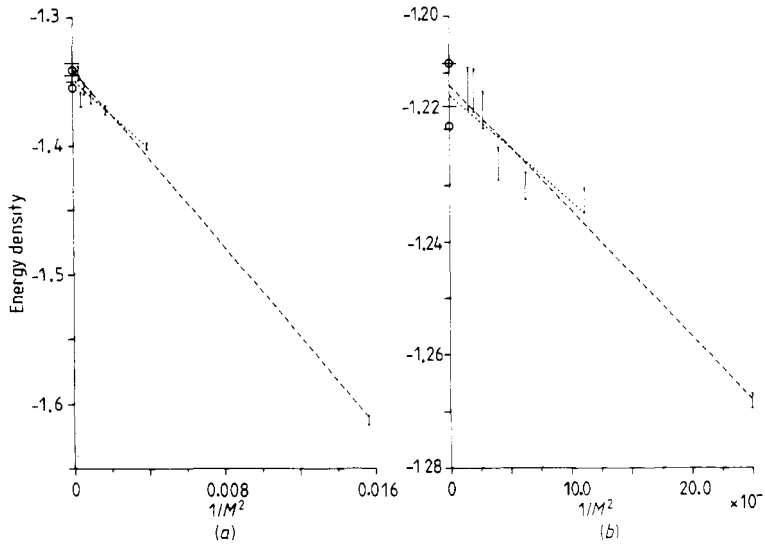

Figure 8. Linear fit for the energy density as a function of $1/M^2$. The broken line is a fit of all data points. The dotted line is a fit of the data points excluding the point with the lowest value of M. The error bars are given at a confidence level of 68%. The bars on the y axis denote the estimated error for the extrapolated value corresponding to the broken line; the circles on the y axis denote the estimated error for the extrapolated value corresponding to the dotted line. Both estimated errors have been obtained by a mean square fit, and are given at a confidence level of 95%. (*a*) $J_z = -1.0$, $\beta = 2.5$; (*b*) $J_z = -0.5$, $\beta = 5.0$.

useful to make the linear fit starting with as small values of M as possible, i.e. from the onset of the asymptotic $1/M^2$ behaviour.

In any Monte Carlo calculation there are numerical problems deriving from the inherent statistical fluctuations of the measured quantities. In order to illustrate how these numerical problems manifest themselves in the linear $1/M^2$ fits, we give in figure 9 some examples of linear fits for $I(q)$. In some cases (figures 9(*c*) and (*d*)) the linear fits do not give a good optical impression. However, such cases will always occur with a certain, albeit small probability. Having the results of several measurements at our disposal (for the several values of M considered) allows for a reasonable extrapolation in these cases too.

We would like to conclude this section by stressing that the $M \to \infty$ extrapolation has to be done for each quantity for each value of the couplings for each temperature. Without an extrapolation procedure the quantum Monte Carlo method does not yield reliable results.

4. Results

We will show here only the results for $S = 1$. Some of our spin-$\frac{1}{2}$ results are given in Honerkamp (1982), where it is shown that they compare favourably with known exact results. Spin-$\frac{1}{2}$ results have been published in Hirsch *et al* (1982) and Schmatzer (1983) (the results given in Schmatzer (1983) for the Thirring model are published in Marcu

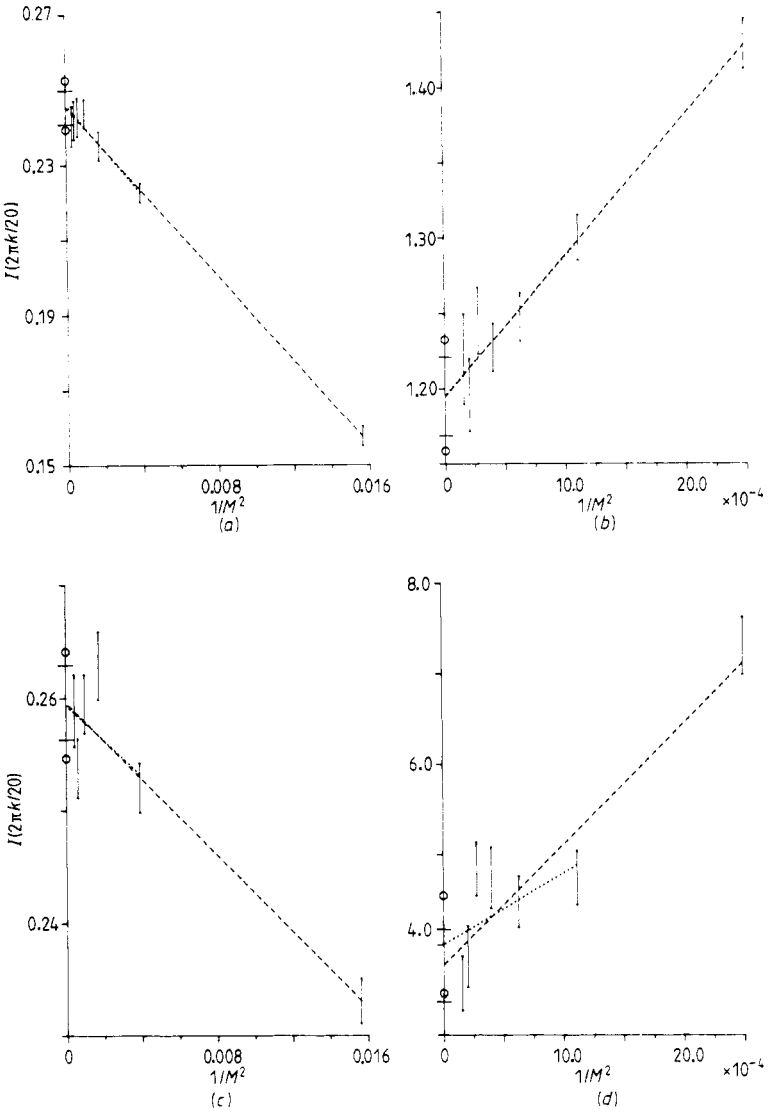

Figure 9. As figure 8, but for the static structure function at four different values of (q, J_z, β). (a) and (b) are two examples of 'optically' very good fits; (c) and (d) are examples of fits where the statistical fluctuations of the Monte Carlo data are considerable. However, in most cases the data allowed for optically good fits. (a) $k=4$, $J_z=-1.0$, $\beta=2.5$; (b) $k=10$, $J_z=-0.5$, $\beta=5.0$; (c) $k=3$, $J_z=-0.5$, $\beta=2.5$; (d) $k=10$, $J_z=-1.0$, $\beta=5.0$.

and Schmatzer (1985)). In Schmatzer (1983) linear $1/M^2$ fits are also used. There the aim is to obtain high accuracy results at very low temperature.

For $S=1$ all our simulations have been done with 5000 sweeps and one measurement after each sweep. The system was thermalised with 2500 sweeps.

As pointed out above, the convergence rate of our approximation on the $N\times M$ lattice varies from one measured quantity to another, and we investigated the $M\to\infty$ limit for each quantity separately. In figure 7 we see that the energy density converges

slower than $I(\pi/2)$. In fact the energy density converges slower than $I(q)$ for all values of q. This is due to the fact that in equations (2.10)-(2.11) the values of $e(p)$ can become very large for $\bar{\beta} \to 0$.

Our results for the energy density as a function of temperature are plotted in figure 10. In figure 10(a) the dotted lines are the results of Wang (1968), obtained by computer diagonalisation of the xxz Hamiltonian for $N = 5$, 6 and 7. In figure 10(b) the lines are drawn to guide the eye. In table 2(a) we list the results for the energy density, and in 2(b) the ground-state energy density (i.e. the zero temperature energy density) for the values of J_z considered here. For $J_z = 1$ the ground-state energy density is easily seen to be -1.0; for the other values of J_z it was computed by Blöte (1975) using a method similar to Wang (1968).

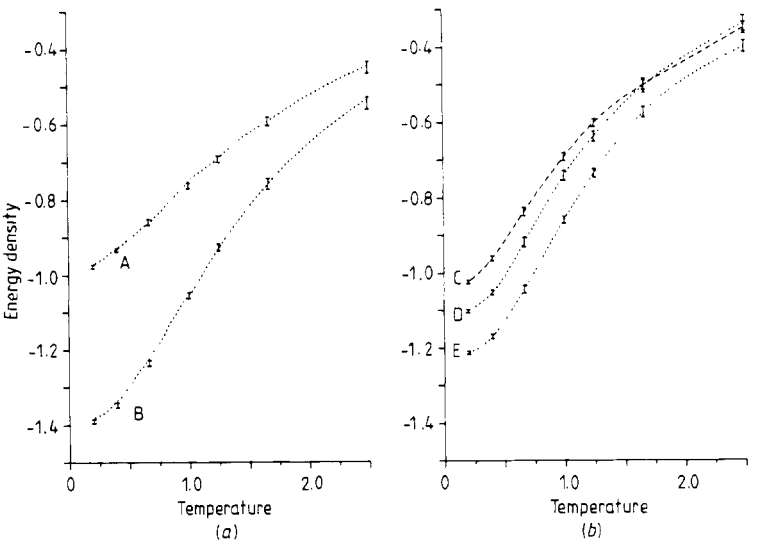

Figure 10. Energy density as a function of temperature. The values of J_z are A, 1.0; B, -1.0; C, 0.5; D, 0; E, -0.5.

In figures 11 and 12 we plotted our results for the s^z-s^z magnetic susceptibility $\beta I(0)$ (figure 11), and for the quantity $\beta I(\pi)$ (figure 12), which for $J_z = -1$ is the staggered susceptibility. The dotted lines are drawn to guide the eye. The accuracy of these results does not allow a quantitative investigation of the critical properties as $T \to 0$. However, many important physical properties are apparent. Thus for $J_z = -0.5$, 0 and 0.5 the susceptibility has a peak at finite temperature and converges to a finite value as $T \to 0$ (figure 11(a)). For $J_z = 1$ the susceptibility diverges as $T \to 0$ (figure 11(b)); the same is true for the staggered susceptibility at $J_z = -1$ (figure 12(b)).

In figure 13 we plotted our results for the static structure function $I(q)$. As stated in the introduction, we kept the lattice size constant ($N = 20$) throughout our calculation. For $J_z = -1$, -0.5, 0 and 0.5 the static structure function has a peak at $q = \pi$. This is a reflection of the antiferromagnetic nature of the ground state. It is interesting to notice that for $J_z = 0.5$ the peak at $q = \pi$ develops only at low temperatures. This is due to the proximity of the ferromagnet.

In order to perform the thermodynamic limit, the value of N has to be increased until $N/2$ is larger than the correlation length (we must take $N/2$ and not N because

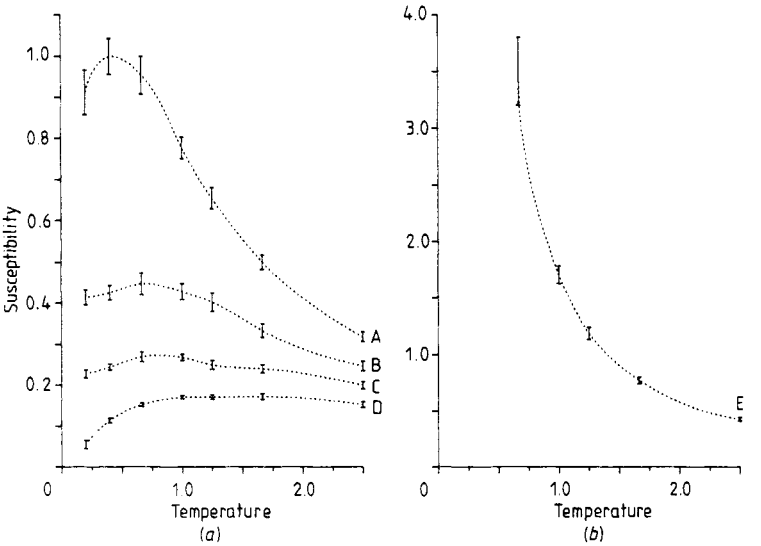

Figure 11. The magnetic susceptibility as a function of temperature. The values of J_z are A, 0.5; B, 0; C, −0.5, D, −1.0; E, 1.0.

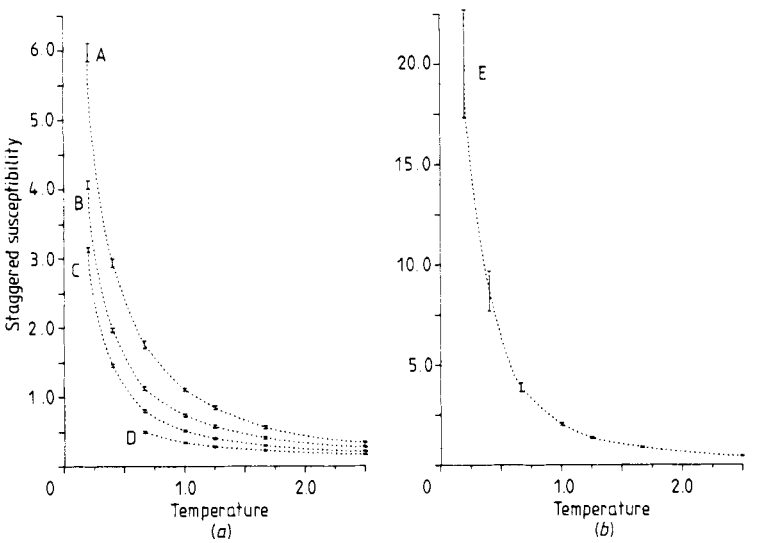

Figure 12. The quantity $\beta I(q)$ as a function of temperature. This quantity is the staggered susceptibility for the values 1 and −1 of J_z. The values of J_z are A, −0.5; B, 0; C, 0.5; D, 1.0; E, −1.0.

of the periodic boundary conditions). For $J_z = -0.5$, 0 and 0.5 the value $N = 20$ fulfilled this requirement for all temperatures considered here. For $J_z = -1$ and 1, however, $N = 20$ was large enough only for temperatures not exceeding $T = 1$ (the correlation length was estimated as the distance where the s^z-s^z correlations became zero within error bars).

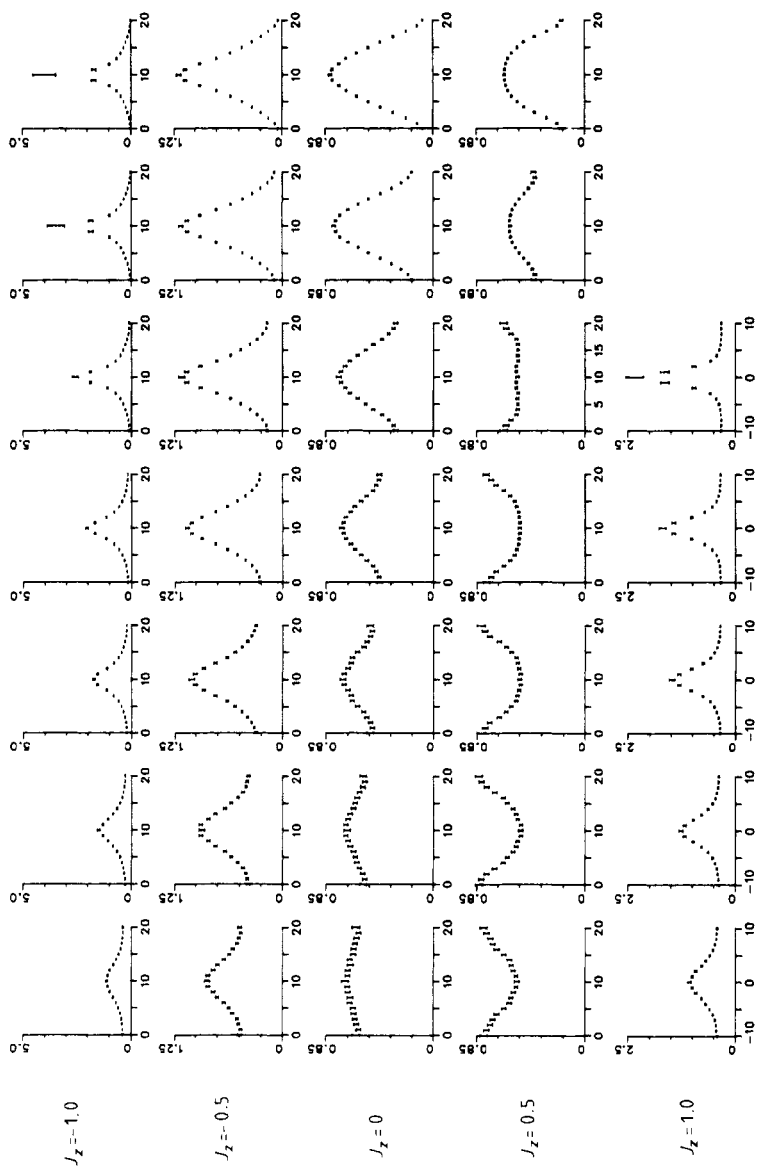

Figure 13. The static structure function $I(2\pi k/N)$ as a function of k.

5. Conclusions and outlook

We have tested a Monte Carlo procedure for the spin S anisotropic Heisenberg (xxz) model at finite temperatures. For every value of the couplings and of the temperature, a Monte Carlo simulation was performed for a sequence of approximating two-dimensional classical systems. The method used for simulating the classical system consists of a local part and a non-local one. Only including the latter allows us to get a sample of all relevant configurations.

For the first time, we included in a quantum Monte Carlo method a systematic procedure for extrapolating the results obtained in the sequence of classical simulations. (The only other attempt to do this is, to our best knowledge, that of Cullen and Landau (1983). Their use of finite size scaling theory is however problematic since the two-dimensional classical system is highly anisotropic with couplings that vary with the lattice size in the Trotter direction.)

In subsequent publications (Marcu *et al* 1985), we plan to deal with the computation of s^x-s^x correlations, computations for xxz chains with external magnetic field, comparison of Monte Carlo results with experiments on one-dimensional materials and with various theoretical predictions (e.g. in xxz models with a crystal field anisotropy term), and simulations of xxz models in more than one dimension, all these for arbitrary spin.

Acknowledgments

We would like to thank Professor J Honerkamp for his constant support and encouragement. One of us (MM) would also like to thank Dr K Fredenhagen and F K Schmatzer for many interesting discussions.

References

Barma M and Shastry B S 1978 *Phys. Rev.* B **18** 3351
Blöte H W J 1975 *Physica* **79B** 427
des Cloizeaux J and Gaudin M 1966 *J. Math. Phys.* **7** 1384
Cullen J and Landau D P 1983 *Phys. Rev.* B **27** 279
Hirsch J E, Sugar R L, Scalapino D J and Blankenbecler R 1982 *Phys. Rev.* B **26** 5033
Honerkamp J 1982 *Lectures given at the Les Houches Summer School on 'Recent advances in field theory and statistical mechanics', August-September 1982*
Marcu M, Müller J and Schmatzer F K 1985 *J. Phys. A: Math. Gen.* **18**
Marcu M and Schmatzer F K 1985 *Preprint, Computation of masses in the Thirring model using a quantum Monte Carlo method* Freiburg
Schmatzer F K 1983 *Diplomarbeit* Freiburg
Suzuki M 1976 *Commun. Math. Phys.* **51** 183
—— 1977 *Prog. Theor. Phys.* **58** 377
Trotter H F 1959 *Proc. Am. Math. Soc.* **10** 545
Wang C Y 1968 *PhD Thesis* Carnegie-Mellon University
Wiesler A 1982 *Phys. Lett.* **89A** 359